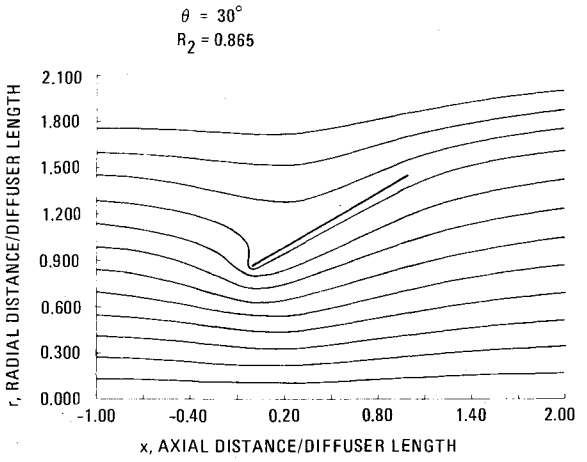

Fig. 2 Upper-half diffuser streamlines for $C_{T_0} = 0.8$.

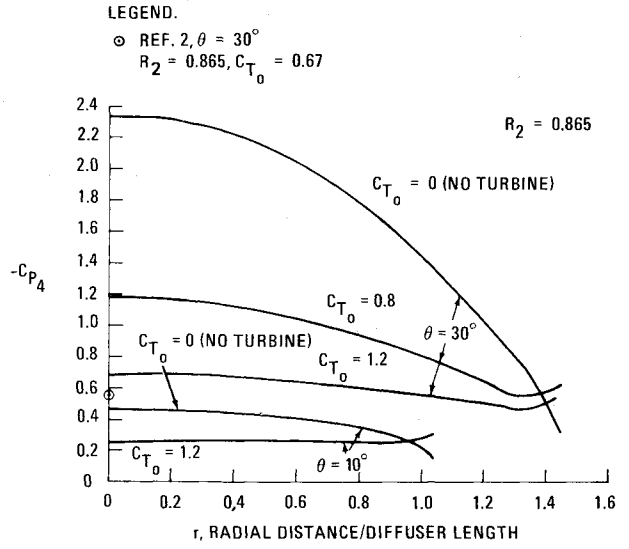

Fig. 3 Pressure coefficient profile in exit plane.

the flowfield is shown, with the abscissa axis ($\psi = 0$) representing the axis of symmetry of the flow. The diffuser wall itself is seen to extend between $x = 0$ and $x = 1.0$. The values of stream function ψ are not indicated in the illustration, but they have been chosen such that the streamlines are equidistant for uniform undisturbed flow (i.e., far upstream or far downstream). It is then easy to determine whether the flow is locally accelerated or retarded by observing whether the streamlines are more or less closely spaced, respectively. The effect of the diffuser in concentrating the flow through the turbine disk is evident in Fig. 2. This effect is explained simply by the circulation produced by the diffuser acting as an annular airfoil, with the inside surface of the diffuser being the high velocity, low pressure side of the airfoil.

In Fig. 3 is shown the variation of the exit plane pressure coefficient with radius. Consistent with the experimental findings of Ref. 2, the static pressure in the exit plane is seen to be subatmospheric (below freestream pressure). The addition of a flow resistance (turbine or screen) at the diffuser entrance has a strong flattening effect on the curves. As expected, the pressure reduction below atmospheric is much greater for the larger angle diffuser. The one experimental datum from Ref. 2 for $\theta = 30$ deg, $C_{T_0} = 0.67$, and $r = 0$ is seen to fall considerably below the value of $-C_{p_4}$ that one would estimate from interpolating the curves. This discrepancy is probably caused by the finite thickness of the wall and the boundary layer control flow and by viscous effects in the experiments that are not accounted for in the theory. The experiments utilized slots for injecting air from the external flow into the diffuser boundary layer to reduce separation, and no attempt was made to model these theoretically.

In conclusion, we have shown that the pressure reduction in the base region behind a wide-angle diffuser and the subsequent enhanced flow through the diffuser can be accounted for qualitatively by inviscid theory. The inviscid predictions are overly optimistic, however, indicating the need to account also for viscous effects for more accurate results.

References

[1] Foreman, K.M., Gilbert, B.L., and Oman, R.A., "Diffuser Augmentation of Wind Turbines," Grumman Research Department paper, presented at International Solar Energy Society Meeting, Winnipeg, Aug. 1976.

[2] Oman, R.A., Foreman, K.M., and Gilbert, B.L., "Investigation of Diffuser-Augmented Wind Turbines," Parts I and II, ERDA Report C00-2616-2, prepared under ERDA Contract No. E(11-1)-2616, August 1976; also published as Grumman Research Department Report RE-534, Jan. 1977.

[3] Igra, O., "Shrouds for Aerogenerator," Ben Gurion University of the Negev, Dept. of Mechanical Engineering, Report No. 2, March 1975.

[4] Kuchemann, D. and Weber, J., *Aerodynamics of Propulsion*, McGraw-Hill, New York, 1953, Chaps. 3,5.

[5] Bagley, J.A., Kirby, N.B., and Marcer, P.J., "A Method of Calculating the Velocity Distribution on Annular Airfoils in Incompressible Flow," R.A.E. Technical Note Aero 2571, Dec. 3, 1958.

[6] Young, C., "A Computer Program to Calculate the Pressure Distribution of an Annular Aerofoil," R.A.E.-TR-71199, Sept. 1971.

[7] Mann, M.J., "Subsonic Annular Wing Theory with Application to Flow About Nacelles," NASA TN-D-7630, Sept. 1974.

[8] Loeffler, A.L., Jr. and Vanderbilt, D., "Inviscid Analysis of Flow Around a Wide-Angle Diffuser with an Internal Actuator Disk," Grumman Research Department Report RE-541, May 1977.

Some Effects of Unstable Resonators on Performance of CW Chemical Lasers

W. J. Glowacki,* K.-Y. Chien,† and W. P. Altman‡
Naval Surface Weapons Center, Silver Spring, Md.

THIS Note presents some computed results showing the effect of various cylindrical confocal unstable resonator configurations on the performance of a CW (continuous wave) chemical laser. These results have been obtained using the non-time-dependent LAMPPOST code[1,2] with the technique described in Ref. 3 for accelerating convergence of the solution. The LAMPPOST code has been developed by coupling Lockheed's Laser and Mixing Program[4,5] (known as the LAMP code) and a physical optics code for unstable resonators. The physical optics code developed by Altman uses the fast fourier transform techniques described by Salvi[6] and Phelps.[7] The effect of density variations on the index of refraction has not been included.

Figure 1 shows schematically the lasing region of a typical CW chemical laser operating with DF. Atomic fluorine and

Presented at the AIAA 10th Fluid and Plasma Dynamics Conference, Albuquerque, N. Mex., June 27-29, 1977 (Open Forum Session, no Preprints); submitted Feb. 27, 1978; revision received June 19, 1978.

Index categories: Lasers; Radiatively Coupled Flows and Heat Transfer.

*Physicist, Applied Mathematics Branch. Member AIAA.

†Research Aerospace Engineer, Applied Mathematics Branch. Associate Fellow AIAA.

‡Electrical Engineer, Radar Engineering Branch.

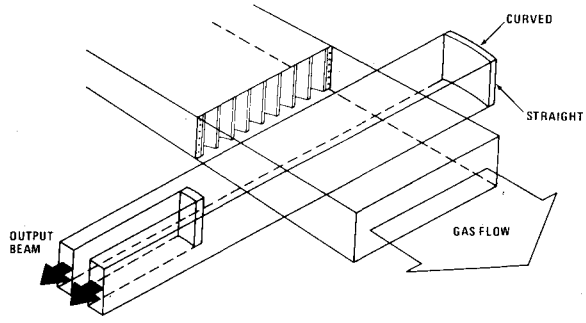

Fig. 1 Schematic diagram of lasing region.

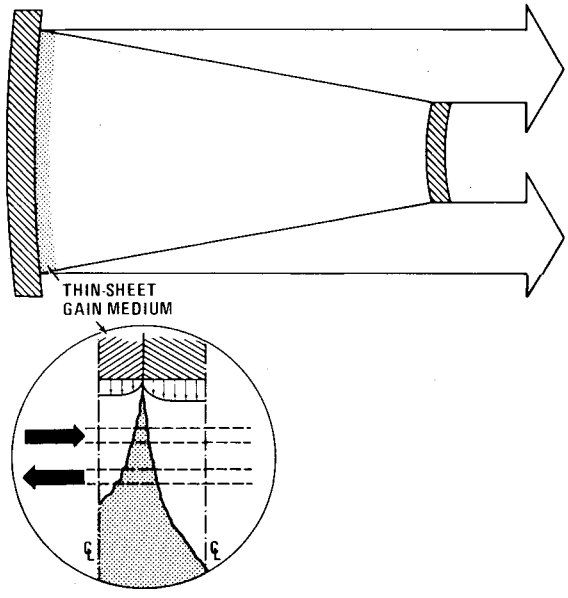

Fig. 2 Schematic diagram illustrating thin-gain-sheet approximation.

deuterium emerging from alternate nozzles mix and react to form vibrationally excited DF. Lasing occurs in the optical cavity formed by appropriately placing mirrors on opposite sides of the flow region. The LAMP code treats in detail the mixing, reacting, and lasing processes occurring in the laser cavity for the case where the mirrors are plane, parallel, and rectangular. Power can be extracted by making one of the mirrors transmit partially. For a number of reasons, which include the difficulties in aligning the mirrors and in withstanding the thermal loading in the transmitting mirror, this is not the best optical configuration for use on a chemical laser device.

Figure 1 illustrates the use of a cylindrical confocal unstable resonator. The mirrors are curved in the flow direction. The smaller, convex mirror is shown in the on-axis position in which it reflects the central portion of the resonator beam. If this mirror is positioned at the upstream or downstream edge of the resonator beam, the unreflected portion will form a single output beam, rather than the two shown in this figure.

Figure 2 illustrates how the usual thin-gain-sheet approximation is used to separate the calculation of one round trip through the resonator into distinct propagation and amplification phases. From the gain sheet, which is assumed to be located at the concave mirror, the beam is propagated across the cavity to the plane of the convex mirror, where the powers in the reflected and output portions of the beam are calculated. The reflected beam is then propagated back across the cavity to the edge of the gain sheet. The beam now passes into and out of the gain sheet completing one round trip. While passing through the gain medium, the beam is amplified. The gas mixture and flow properties and the gain and

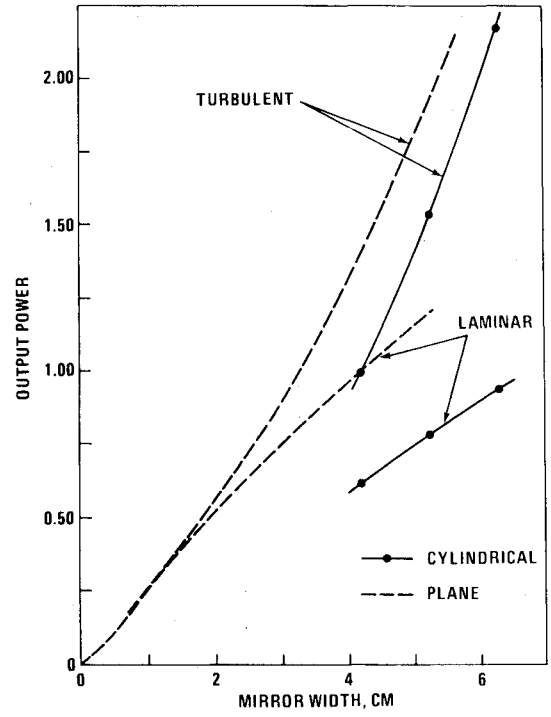

Fig. 3 Comparison of unstable resonator and plane mirror configurations for laminar and turbulent flows.

outgoing (amplified) beam distributions are calculated using a modified LAMP code which accepts a specified incoming beam distribution. If this amplified beam distribution matches the one used to begin the propagation phase of the calculation, the solution has been found. If not, additional round-trip calculations are made until the results converge to the desired degree. This approximation of lumping the distributed gain in the cavity into one or more thin sheets has been used widely before and appears valid for the cases considered. Other authors have also included index of refraction variations into this approximation, but inclusion of these effects into two-dimensional calculations was not deemed realistic.

A base case[1] representative of current DF chemical lasers was used to calculate the effect of various resonator parameters. Figure 3 shows the effect of resonator width on the output power for an on-axis unstable resonator with 60% geometric output coupling and located right at the nozzle exit plane. Results are shown both for a turbulent flow with moderate initial turbulence levels and for a flow which remains laminar. For these cases, the optimum resonator width has not yet been reached. For comparison, the dashed curves indicate the normalized power output predicted by the LAMP code for plane mirrors of various widths. The results show that the plane mirror analysis of LAMP predicts significantly higher output powers than the unstable resonator analysis of LAMPPOST. For the resonator and flow conditions of the base case, the overprediction is about 40%. This overprediction occurs because, in the plane mirror analysis, lasing occurs on the line in each vibrational band which has the maximum gain locally, i.e., at that particular streamwise location. In the unstable resonator analysis, lasing occurs on the line in each vibrational band which has the maximum gain over the whole gain region.

Calculations were also made to illustrate the effect of varying the position of the resonator's optical axis. As the optical axis moves downstream, away from the nozzle exit, the output power increases, reaching a maximum in the vicinity of the on-axis position and then decreasing only slightly thereafter. For these calculations, the maximum loss of output power for various positions of the optical axis is

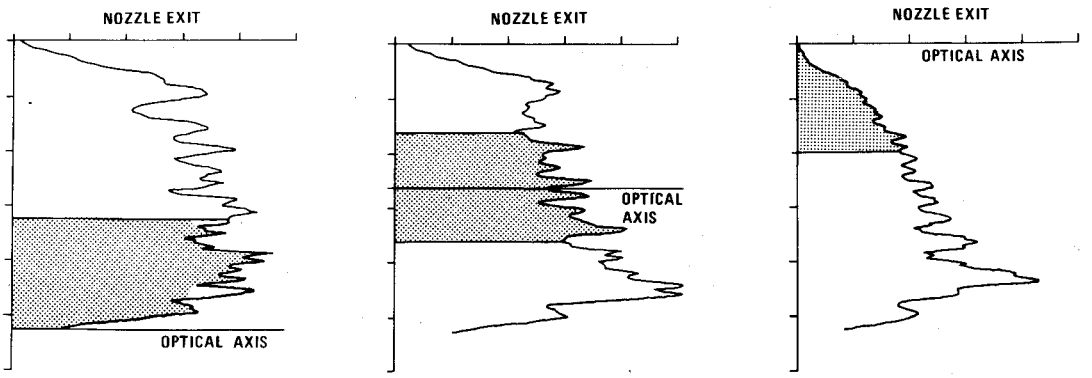

Fig. 4 Total intensity distributions at output end of resonator for three optical axis locations.

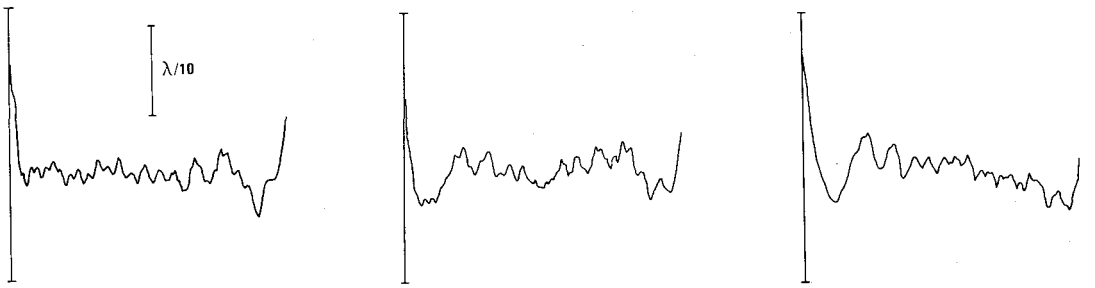

Fig. 5 Phase distributions at output end of resonator corresponding to intensity distributions of Fig. 4.

about 13% and occurs when the optical axis is at the nozzle exit plane (NEP). If the optical axis is more than about one-fourth of the way downstream from the NEP, there is little effect on the calculated output power. This general behavior is consistent with previous experimental results,[8] even though the gain characteristics are different.

Figure 4 shows the total intensity distributions across the beam for three positions of the optical axis relative to NEP. The unshaded portion is the output beam from the resonator. The topmost distribution corresponds to the case where the optical axis is at the NEP; the intensity distribution is highly skewed in the downstream direction. As the optical axis is moved downstream to the on-axis position (i.e., optical axis normal to the center of the concave mirror), the skewness decreases. When the optical axis reaches its most downstream position, the intensity is distributed reasonably uniformly across the beam width. Phase plots for these configurations are shown in Fig. 5 in the same order as Fig. 4. Only one phase plot is given for each configuration, because the phase distribution is virtually identical for any line with a reasonable ($>3\%$) percentage of the total power. The ripples that appear are mostly due to high Fresnel number of the cavity modeled. Even with the large number of oscillations in the phase profile, the variations are confined to a region less than $\lambda/10$. Considering the design of the optical components and beam propagation, configurations such as the one with optical axis downstream of the on-axis position, which give a relatively uniform output distribution without the typical hole-in-the-center characteristic of on-axis resonators, may be more desirable provided there is little loss in output power. Further examination of the relative merits of the different configurations would require far-field diffraction calculations including the effects of atmospheric absorption (i.e., thermal blooming).

References

[1] Glowacki, W. J., Chien, K.-Y., Altman, W. P., and Heiche, G.F.A., "LAMPPOST, a CW Chemical Laser Mixing Code for Unstable Resonators, I. Concept, Formulation, and Initial Results," Naval Surface Weapons Center, White Oak Laboratory, Silver Spring, Md., NSWC/WOL/TR 76-168, Dec. 1976.

[2] Chien, K.-Y. and Glowacki, W. J., "LAMPPOST, a CW Chemical Laser Mixing Code for Unstable Resonators, II. User's Guide for 2D, On-Axis Resonators," Naval Surface Weapons Center, White Oak Laboratory, Silver Spring, Md., NSWC/WOL/TR 76-169, Dec. 1976.

[3] Chien, K.-Y. and Glowacki, W. J., "Accelerating Convergence of Unstable Resonator Calculations with a Gain Medium." *AIAA Journal*, Vol. 16, June 1978, pp. 627-628.

[4] Thoenes, J. and Ratliff, A. W., "Chemical Laser Analytical Model," AIAA Palm Springs, Calif., Paper 73-644, July 1973.

[5] Thoenes, J., McDanal, A. J., Ratliff, A. W., and Smith, S. D., "Analysis of Chemical Lasers, Volume 1. Laser and Mixing Program (LAMP), Theory and User's Guide," Lockheed Missiles and Space Company, Huntsville, Ala., MICOM Report RK-CR-74-13 (also LMSC-HREC TR D390222-I), June 1974.

[6] Salvi, T. C., "A Description and Comparison of Methods for Computing Diffraction Integrals," Air Force Weapons Laboratory, Albuquerque, N. Mex., AFWL-TR-74-344, Jan. 1975, pp. 71-79.

[7] Phelps, D., "A New Laser Propagation Algorithm Using the Fast Fourier Transform," Air Force Weapons Laboratory, Albuquerque, N. Mex., AFWL-TR-74-344, Jan. 1975, pp. 80-83.

[8] Phillips, E. A., Reilly, J. P., and Northam, D. B., "Off-Axis Unstable Laser Resonator: Operation," *Applied Optics*, Vol. 15, Sept. 1976, pp. 2159-2166.